Comparison of Water-Soluble CdTe Nanoparticles Synthesized in Air and in Nitrogen

Yuanfang Liu,[†] Wei Chen,*[,†,‡] Alan G. Joly,[§] Yuqing Wang,[||] Carey Pope,[⊥] Yongbin Zhang,[⊥] Jan-Olov Bovin,[#] and Peter Sherwood[||]

Nomadics, Inc., 1024 South Innovation Way, Stillwater, Oklahoma 74074, Department of Physics, The University of Texas at Arlington, Arlington, Texas 76019, Pacific Northwest National Laboratory, P.O. Box 999, Richland, Washington 99352, Department of Physics, Oklahoma State University, Stillwater, Oklahoma 74078, Department of Physiological Sciences, Oklahoma State University, Stillwater, Oklahoma 74078, and Materials Chemistry, Lund University, P.O. Box 124, SE-22100, Lund, Sweden

Received: May 19, 2006; In Final Form: July 5, 2006

It is commonly believed that high-quality CdTe nanoparticles with strong luminescence can only be prepared under the protection of an inert gas such as nitrogen or argon. Here, we report the preparation of highly luminescent CdTe nnaoparticles in air and compare their luminescence properties with CdTe nanoparticles made in nitrogen. We find that both water-soluble CdTe nanoparticles made in air and in nitrogen exhibit strong photoluminescence as well as upconversion luminescence at room temperature. However, differences do exist between the particles made in air and those made in nitrogen. In particular, the particles prepared in air display a faster growth rate, grow to larger sizes, and display stronger electron coupling relative to the particles prepared in nitrogen. X-ray photoelectron spectroscopy analysis indicates that the oxygen content in the nanoparticles synthesized in air is higher that that in particles synthesized in N_2, likely resulting in a higher availability of excess free cadmium. Cytotoxicity measurements reveal that the particles made in air appear slightly more toxic, possibly due to the excess of free cadmium.

1. Introduction

CdTe nanoparticles have been the subject of numerous investigations. Because of high quantum efficiency and multicolor availability, CdTe nanoparticles can find applications in solid-state lighting, displays, optical communications, sensors, as well as in biological imaging and detection.[1] Currently, two synthesis strategies, nonaqueous synthesis and aqueous synthesis, are used to prepare CdTe nanoparticles. As compared to the nonaqueous synthesis, aqueous synthesis is more reproducible, cheaper, less toxic, and the "as-prepared" samples are more water-soluble and bio-compatible.[2]

Water-soluble semiconductor nanoparticles can be obtained mainly by two different methods. The first way is to replace the surface-capping molecules on the particles prepared by the TOPO (trioctylphosphine oxide) method with water-soluble thiols or a silica shell.[3−6] However, after the substitution of the surface-capping molecules by hydrophilic molecules, the nanoparticle photoluminescence decreases markedly.[3,7,8] The second method is to directly synthesize semiconductor nanoparticles in aqueous solution using water-soluble stabilizers such as thiols.[2,8,9] The second method has become a popular recipe for making water-soluble nanoparticles. It is generally believed that the preparation should be conducted in inert or reduced atmospheres because oxygen in the air can oxidize the nanoparticles and quench the luminescence. However, high-quality CdSe quantum dots have been prepared using organic solvents both in air and in an inert atmosphere.[10] In our work, we find that highly luminescent water-soluble CdTe nanoparticles can be synthesized in air and their luminescence efficiency is comparable to or higher than that of particles made in nitrogen. In this article, we compare the structural, optical, and cytotoxic properties of CdTe nanoparticles made under similar conditions but using either nitrogen or air atmospheres during preparation.

2. Experimental Section

2.1. Synthesis. 3-Mercaptopropionic acid (MPA, 99%), $Cd(ClO_4)_2$, $NaBH_4$ (96%), and tellurium powder (99.999%, about 200 mesh) were obtained from Sigma, Inc. Ultrapure water with 18.2 MΩ/cm (Millipore Simplicity) was used in all syntheses.

The method for the preparation of NaHTe is described elsewhere,[11,12] with a few modifications. Briefly, 100 mg of sodium borohydride was transferred to a small flask, and 2.5 mL of D.I. water was added. After 40 mg of tellurium powder was added to the flask, the reacting flask was rapidly sealed via a rubber plug with a small long syringe pinhead inserted into the flask to discharge pressure from the resulting hydrogen. After 3−8 h, depending on the diameter size of syringe, the black tellurium powder disappeared and a white sodium tetraborate precipitate appeared at the bottom of the flask. The resulting clear pink or colorless aqueous solution was then transferred carefully into 50 mL of degassed water.

A series of aqueous colloidal CdTe solutions were prepared using the reaction between Cd^{2+} and the NaHTe solution similar to the method described elsewhere.[12] Cd precursor solutions were prepared by mixing a solution of $Cd(ClO_4)_2$ and stabilizer (MPA) solution, and adjusted to different pH values with 2 M NaOH to pH = 8−8.2. The typical molar ratio of Cd:Te:MPA

* Corresponding author. E-mail: weichen@uta.edu.
[†] Nomadics, Inc.
[‡] The University of Texas at Arlington.
[§] Pacific Northwest National Laboratory.
[||] Department of Physics, Oklahoma State University.
[⊥] Department of Physiological Sciences, Oklahoma State University.
[#] Lund University.

10.1021/jp063085k CCC: $33.50
Published on Web 08/09/2006

was 2:1:4.8 in our experiments. This solution was placed in a three-necked flask and was degassed with N_2 bubbling for more than 30 min to prepare the nitrogen-protected samples. Under vigorous stirring, the prepared oxygen-free NaHTe solution was injected. The resulting solution mixture was heated to 100 °C and refluxed at different times to control the size of CdTe nanoparticles. Aliquots of the reaction solution were taken out at regular intervals for further fluorescence spectra characterization. The procedure for making CdTe particles in air is the same except that no inert gas is used for protection.

2.2. Characterization. Room-temperature optical absorption spectra were taken with a Hewlett-Packard HP8453 spectrophotometer. The photoluminescence excitation and emission were recorded on a SPEX FLUOROLOG fluorescence spectrophotometer. The up-conversion emission spectra and power dependences were collected using a nanosecond optical parametric oscillator/amplifer (Spectra-Physics MOPO-730) operating at a 10 Hz repetition rate and tunable between 440 and 1800 nm. The laser output was directed onto the particles, and emission was collected at right angles to the excitation and focused into a 1/8-meter monochromator equipped with a gated intensified CCD detector. The power dependences were measured by integrating the area under the luminescence peaks as a function of input power. The lifetimes were collected using the output of a femtosecond regeneratively amplified titanium: sapphire laser system operating at 1 kHz. The 150 fs pulses of this laser at either 830 nm (for upconversion luminescence) or else the second harmonic at 415 nm (for photoluminescence) were directed onto the particles, and the emission was collected at right angles and focused into a streak camera (Hamamatsu C5680). Suitable band-pass and cutoff filters were used to collect the luminescence at different wavelengths. The time resolution was determined to be about 200 ps fwhm using a standard scattering material.

The compositions of the nanoparticles were determined by X-ray photoelectron spectroscopy (XPS). All spectra reported were recorded on a SPECS Stage 100 spectrometer operation in the fixed analyzer transmission (FAT) mode using achromatic Mg Kα (1253.6 eV) radiation at 290 W (12 kV and 20 mA) derived from a water-cooled X-ray gun. The base pressure of the chamber was $\sim 2 \times 10^{-8}$ Torr, the energy scales were calibrated using copper, and the separation between photoelectron peaks was generated by Mg and Al Kα X-rays. Survey spectra were collected with a pass energy of 30 eV; a pass energy of 15 eV was used for both core and valence band spectra. Spectra were calibrated by taking the C1s peak due to residual hydrocarbon as being at 284.6 eV.

2.3. Cytotoxicity Evaluation. Human hepatoma HepG2 cells obtained from American Type Culture Collection were maintained at 37 °C (5% CO_2, 95% air) in Dulbecco's Modified Eagles Medium (Sigma) containing 10% fetal bovine serum (Hyclone) and 1.5 g/L sodium bicarbonate. Confluent cells were harvested with 0.25% trypsin-EDTA solution (Sigma) and seeded into 96-well cell culture plates at a density of 2×10^5 cells/mL for measurement of mitochondrial viability using the MTT assay. Cells were allowed to attach for 24 h before treatment with CdTe nanoparticles. The stock solution of CdTe nanoparticles was sterilized using a 0.22 μm filter. Prior to addition of nanoparticles, the medium was replaced, and then nanoparticles were added to yield final concentrations of 0, 10^{-8}, 10^{-7}, 10^{-6}, and 10^{-5} M. Cells were then placed back into the incubator for 24 h before conducting the MTT assay.

The colorimetric MTT assay is based on the ability of the mitochondrial succinate−tetrazolium reductase system to convert the yellow dye (MTT) to a blue formazan product. Following incubation with nanoparticles, the medium (100 μL/well) was aspirated and replaced by serum-free medium. A stock solution of MTT (5 mg/mL, 10 μL) was added to each well followed by incubation for 4 h at 37 °C. The supernatant was then removed, and cells were lysed with 100 μL of DMSO. Absorbance was recorded at 550 nm using a microplate reader (Wallace 1420 Victor 2, Perkin-Elmer Inc.).

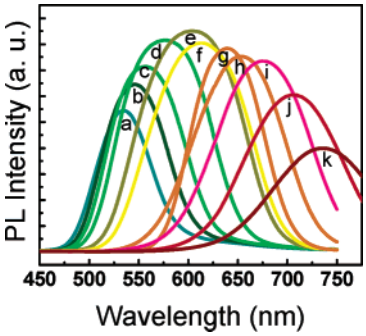

Figure 1. The 400 nm excited emission spectra of CdTe nanoparticles prepared in air at different reaction times: (a) 1.5 h, $\lambda_{max} = 535$ nm; (b) 2.5 h, $\lambda_{max} = 546$ nm; (c) 3.5 h, $\lambda_{max} = 557$ nm; (d) 5.5 h, $\lambda_{max} = 576$ nm; (e) 6.5 h, $\lambda_{max} = 605$ nm; (f) 7.5 h, $\lambda_{max} = 614$ nm; (g) 8.5 h, $\lambda_{max} = 640$ nm; (h) 9.5 h, $\lambda_{max} = 656$ nm; (i) 11.5 h, $\lambda_{max} = 677$ nm; (j) 14.5 h, $\lambda_{max} = 707$ nm; (k) 17.5 h, $\lambda_{max} = 737$ nm.

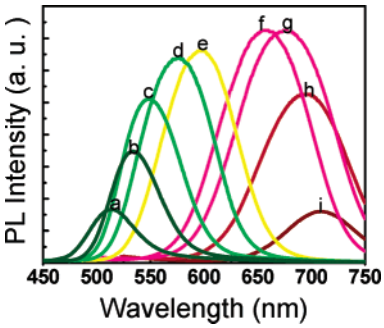

Figure 2. The 400 nm excited emission spectra of CdTe nanoparticles prepared in nitrogen at different reaction times: (a) 1 h, $\lambda_{max} = 515$ nm; (b) 2 h, $\lambda_{max} = 535$ nm; (c) 3.5 h, $\lambda_{max} = 557$ nm; (d) 6.5 h, $\lambda_{max} = 576$ nm; (e) 8 h, $\lambda_{max} = 597$ nm; (f) 18 h, $\lambda_{max} = 659$ nm; (g) 22.5 h, $\lambda_{max} = 675$ nm; (h) 26.5 h, $\lambda_{max} = 695$ nm; (i) 29 h, $\lambda_{max} = 708$ nm.

3. Results and Discussion

3.1. Optical Absorption and Emission Spectra. Figure 1 displays the typical photoluminescence spectra of MPA-stabilized CdTe nanoparticles prepared in air. At the nucleation stage after the injection of the NaHTe solution, there is no luminescence observed from the solution. As the solution heats to 100 °C in about 40 min, the color of the colloid solution becomes greener and the solution emits a weak green luminescence under UV light. After about 1.5 h of reaction, the fluorescence peak is at 535 nm. As the reaction proceeds, the emission shifts to longer wavelengths. The aliquot with emission maximum at 605 nm approached the highest fluorescence intensity. After about 18 h of reaction, the emission of the CdTe particle solution reached the longest wavelength peaking at 737 nm. Meanwhile, the luminescence intensity becomes weaker and the width becomes broader.

Figure 2 displays the typical photoluminescence spectra of MPA-stabilized CdTe nanoparticles prepared in nitrogen. Similar to the solution made in air, there is no luminescence observed at the nucleation stage after the injection of the NaHTe solution. As the solution heats to 100 °C in about 40 min, the color of

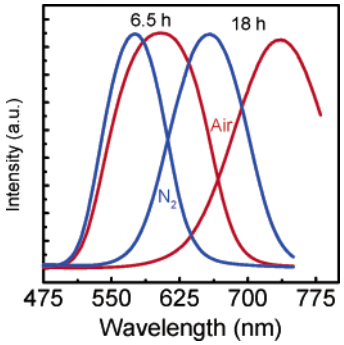

Figure 3. The 400 nm excited emission spectra of CdTe nanoparticles made in air (red) and in nitrogen (blue) at the reaction times of 6.5 and 18 h, respectively.

TABLE 1: Absorption and Emission Wavelengths of Green and Yellow Particles Made in Air and in N_2

	in air		in N_2	
	green	yellow	green	yellow
absorption (nm)	458	516	488	537
emission (nm)	534	576	533	576
Stokes shift (nm)	76	60	45	39
$I_{emission}/I_{absorption}$	135	143	78	118
S	7.54	5.95	4.47	3.87

the colloid solution becomes greener and the solution emits a weak green luminescence under UV light. After about 1.5 h of reaction, the fluorescence peak is at 515 nm. The aliquots with emission peaks at 659 and 675 nm approached the highest fluorescence intensity. After about 29 h of reaction, the emission of the CdTe particle solution reached the longest wavelength peaking at 675 nm. Meanwhile, the luminescence intensity becomes weaker and the width becomes broader.

In our measurements, we find that on average the luminescence intensity of the particles made in air is about 1.2−1.4 times stronger than that of the particles made in nitrogen. The luminescence quantum efficiency is proportional to the emission intensity but inversely proportional to the absorption intensity or absorbance. Therefore, the ratio of the emission intensity to the absorbance can be used to compare the relative efficiencies of the samples. The ratios of the emission intensity excited at 400 nm to the absorbance at 400 nm are given in Table 1 for the green and the yellow particles made in air and in nitrogen. The results show that the ratios for particles made in air are higher than those of the particles made in nitrogen. This demonstrates further that the particles made in air have luminescence efficiencies comparable to or stronger than those of the particles made in nitrogen.

Figure 3 compares the emission spectra of the nanoparticle samples obtained at reaction times of 6.5 and 18 h, respectively. After the same reaction time, the particles made in air have longer emission wavelengths than the particles made in nitrogen. This demonstrates that the nanoparticles made in air grow faster than the particles prepared in nitrogen atmosphere. This is a very interesting observation because for biological in vivo applications, long wavelength emission in the near-infrared window from 700 to 1100 nm is required.[13] This may provide a good recipe for making CdTe nanoparticles for biological applications.

Figures 4 and 5 show the absorption and emission spectra of the green, yellow, and red particles prepared in air and nitrogen, respectively. In both the particles made in nitrogen and air, the green and yellow particles have strong emission and pronounced exciton absorption peaks. However, the red particles show no

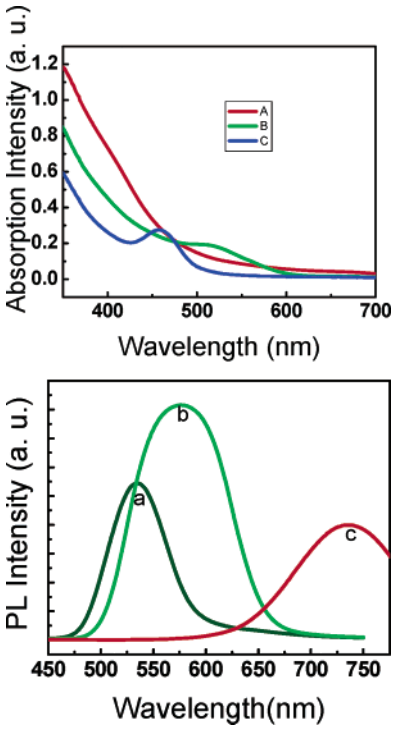

Figure 4. Absorption (top) and emission (bottom) spectra of three samples made in air with emission peaks at (a) 535 nm, (b) 575 nm, and (c) 737 nm.

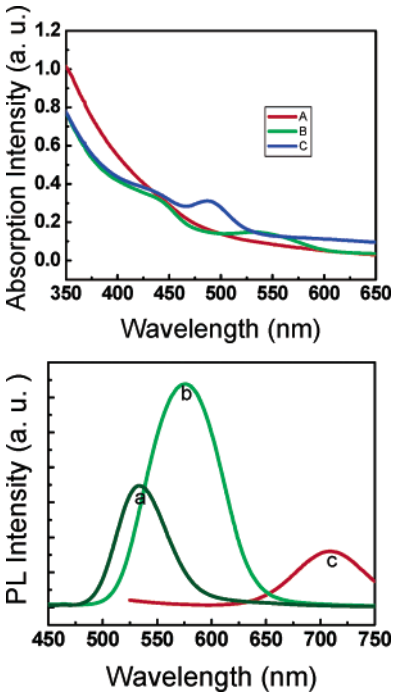

Figure 5. Absorption (top) and emission (bottom) spectra of three samples made in nitrogen with emission peaks at (a) 525 nm, (b) 575 nm, and (c) 708 nm.

obvious exciton absorption peak, and their luminescence is relatively weak. This may be attributed to two possible causes. One is that the size distribution in the red particles is broad, and the other is that the quantum size confinement is weaker. Consequently, their luminescence intensity is weaker than the other particles, and they do not show pronounced exciton absorption peaks.

Table 1 displays the absorption and emission wavelengths of green and yellow particles made in air and N_2, respectively.

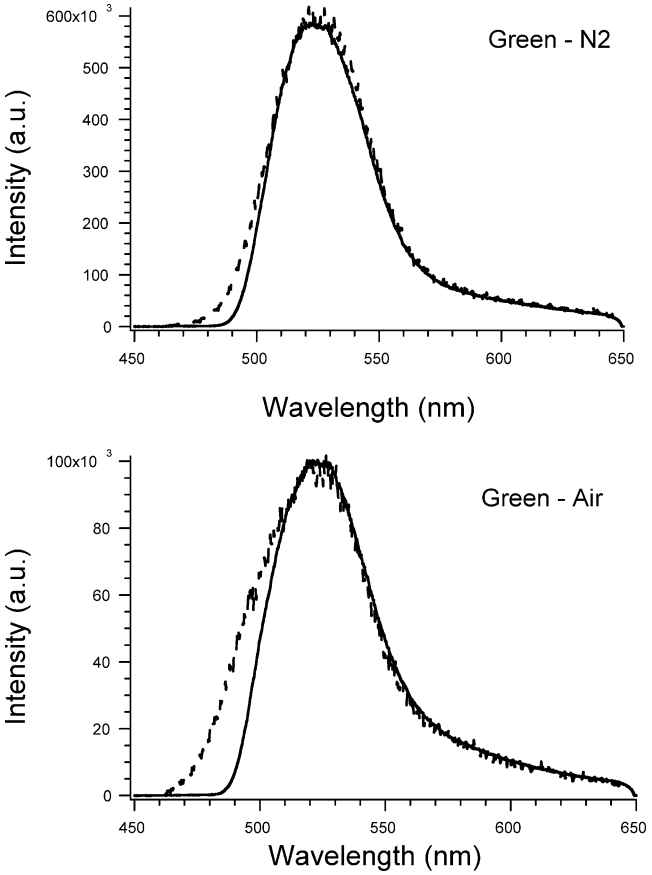

Figure 6. The photoluminescence (solid, excitation at 415 nm) and upconversion (dashed, excitation at 781 nm) luminescence spectra of the green nanoparticles made in nitrogen (top) and in air (bottom).

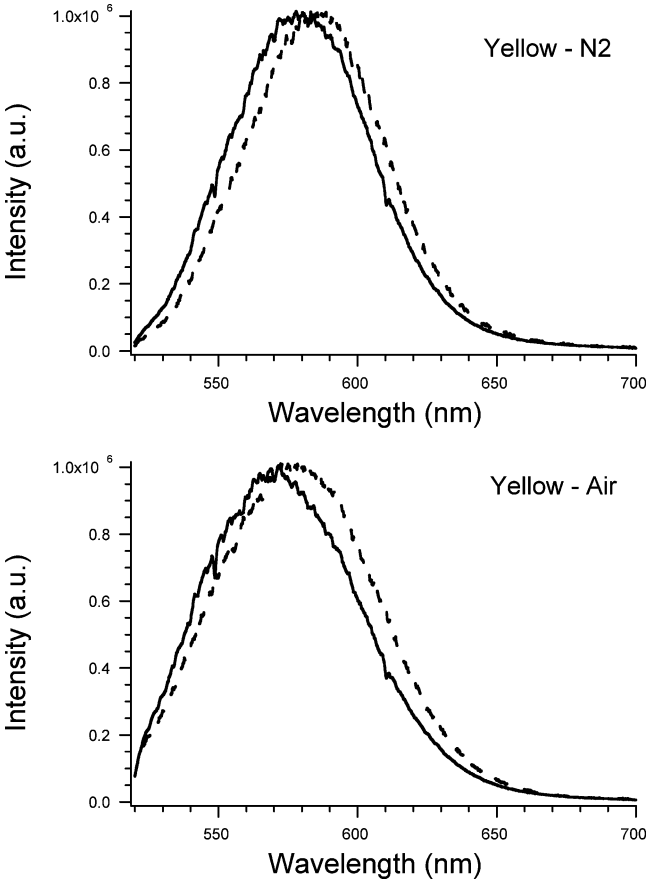

Figure 7. The photoluminescence (solid, excitation at 415 nm) and upconversion (dashed, excitation at 781 nm) luminescence spectra of the yellow nanoparticles made in nitrogen (top) and in air (bottom).

For both green and yellow particles, the Stokes shifts are larger for the particles made in air. This implies that the phonon coupling is stronger in the particles prepared in air.

Exciton−phonon interactions are of considerable importance in semiconductor optics. In semiconductor crystals, exciton−phonon interactions determine the shape of absorption and emission spectra. The role of exciton−phonon interactions in nanoparticles is of great importance as well. In nanoparticles, not only the electronic energy levels but also the lattice modes become discrete due to the three-dimensional confinement.[14] Contrary to bulk crystals, exciton−phonon coupling in nanoparticles does not determine the integral exciton absorption because of negligible exciton−phonon coupling when the particle size is much smaller than the light photon wavelength, that is, $a \ll \lambda$.[15] However, phonons still control the intrinsic dephasing[16] and energy relaxation processes and therefore determine the absorption and emission line widths as well as the luminescence Stokes shift.[15]

A strong electron−phonon coupling may result in a broad emission width and a large Stokes shift. The Huang−Rhys parameter S is a good parameter for evaluating phonon coupling strength.[17] S may be estimated from the Stokes shift Δ_{Stokes}:

$$\Delta_{\text{Stokes}} = 2S\hbar\omega_{\text{LO}} \quad (1)$$

where ω_{LO} is the LO-phonon frequency and $\hbar$ is Planck's constant. For CdTe, $\hbar\omega_{\text{LO}} = 170\ \text{cm}^{-1}$.[18] The Huang−Rhys parameters estimated from the Stokes shifts for the green and yellow nanoparticles prepared in air are 7.54 and 5.95, while the green and yellow particles prepared in nitrogen are 4.47 and 3.87, respectively.

The above results indicate that the phonon coupling in the green nanoparticles is stronger than that in the yellow particles, and the coupling is stronger in the particles made in air than the particles made in nitrogen.

3.2. Upconversion Luminescence and Decay Lifetimes. Upconversion luminescence (UCL) is luminescence in which the emitted wavelength is shorter (higher in energy) than the excitation wavelength in contrast to photoluminescence (PL), where the emitted wavelength is lower in energy than the excitation photons. Intense upconversion luminescence has been observed in aqueous CdTe nanoparticles prepared in inert atmosphere[19] and in organic solvents.[20] For the aqueous CdTe nanoparticles prepared in a nitrogen atmosphere, it was found that the upconversion is due to two-photon excitation.[19] This is of significant importance for applications, particularly for biological imaging, because two-photon optical imaging has several obvious advantages over fluorescence imaging.[21] Advantages arise from the use of infrared wavelengths, thus avoiding tissue auto-fluorescence and increasing the tissue penetration depth.[21] Consequently, more sensitive and higher resolution imaging or detection may be obtained. In addition, two-photon excitation minimizes tissue photodamage, phototoxicity, and photobleaching, as it limits the region of photointeraction to a sub-femtoliter volume at the focal point.

We measured the upconversion luminescence of CdTe nanoparticles prepared in air to evaluate their luminescence properties in comparison with CdTe particles prepared in nitrogen. Figures 6 and 7 display the photoluminescence (excited at 415 nm) and the upconversion emission spectra (excited at 781 nm) of the green and the yellow nanoparticles prepared in air and nitrogen, respectively. For both the particles made in

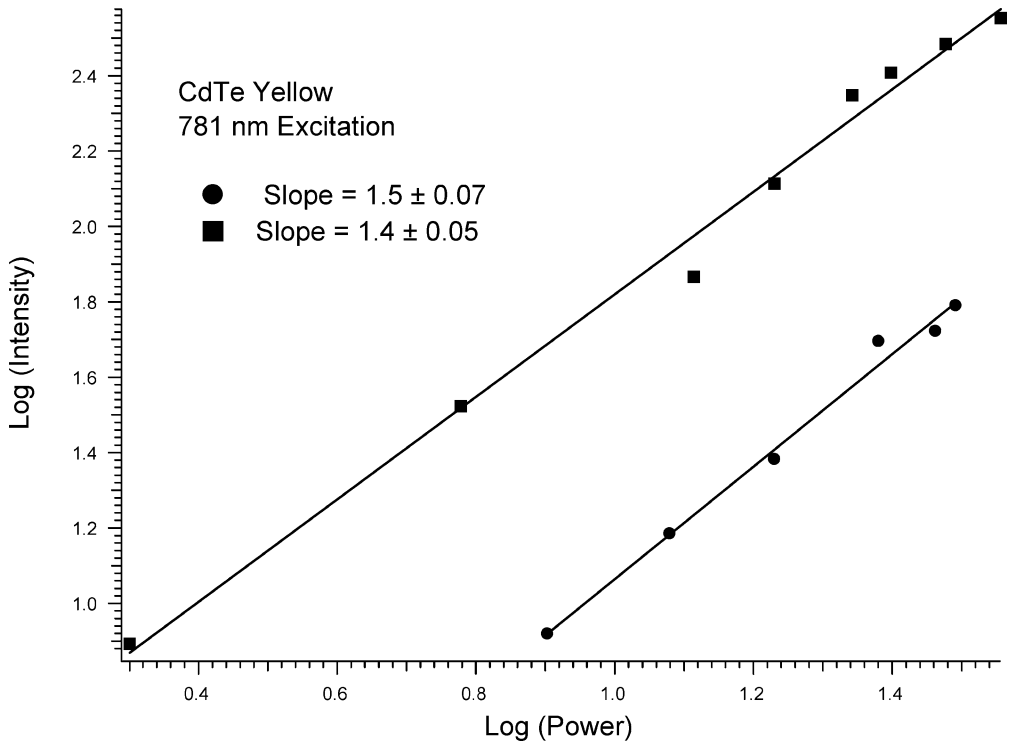

Figure 8. A semi-logarithmic base 10 (Log_{10}) plot of the power dependences of the upconversion emission intensity on laser power at room temperature for yellow CdTe nanoparticles made in air (●) and in nitrogen (■).

air and in nitrogen, upconversion luminescence is observed under the same conditions. For the green nanoparticles, the upconversion emission spectra are almost identical to the photoluminescence emission spectra. However, for the yellow nanoparticles, the upconversion emission peaks are about 5 nm red-shifted from the photoluminescence emission peaks. This result is similar to the upconversion luminescence reported in CdTe[19] and CdSe nanoparticles.[22] The red-shift of the upconversion emission peak relative to the photoluminescence peak is likely due to the involvement of surface defects or/and more contribution of slightly larger particles in the upconversion process.[19,22]

The upconversion mechanism in nanoparticles is still an issue of debate. Often the dependence of the UCL on the input photon power dependence can yield some insight into the mechanism. A semilogarithmic plot displaying the excitation laser power dependences of the upconversion luminescence intensity is displayed in Figure 8 for the yellow nanoparticles. Using the relation of $I \approx \text{Power}^K$, where I is the intensity of the luminescence and Power represents the input laser excitation power, the values of K are 1.5 for the particles prepared in air and 1.4 for the particles prepared in nitrogen. This indicates that the upconversion mechanism in the two particles prepared in air and in nitrogen is the same, most likely due to two-photon excitation. The nonquadratic power dependences may result from either competition between linear and quadratic processes or else saturation of the nonlinear process.[19,22]

The luminescence lifetimes of both the PL and the UCL measured at or near the peak emission are displayed in Figure 9, with the results tabulated in Table 2. The luminescence from all of the solution samples, either made in air or in nitrogen, is nearly single exponential. The green nanoparticles have shorter lifetimes than the yellow nanoparticles in both cases. For the yellow particles, the particles made in air have slightly longer decay lifetimes than the particles made in nitrogen. However, for the green nanoparticles, the decay lifetimes are almost the same for preparation in air and in nitrogen. In all cases, the upconversion decay lifetimes are a little longer than the photoluminescence decay lifetimes; however, the differences are negligible within the experimental error. Overall, the decay properties of the nanoparticles made in air and in nitrogen are very similar. Thus, the quality of the particles made in air can be as high as that of the particles made in nitrogen.

3.3. XPS of CdTe Nanoparticle Samples. Core and valence band XPS was used to investigate the surface chemistry of the nanoparticle samples. This technique provides chemical information about the outer surface region (no more than the top 100 Å of the surface region). XPS analysis can also be used to obtain an estimate of the atomic ratios for the surface region based upon the significant approximation that the surface region is homogeneous over the depth probed by XPS. The trends in the spectra obtained for samples prepared under different conditions will be briefly discussed. The area of a core XPS peak is proportional to the amount of the atomic species in a particular chemical environment. The actual area depends on a number of factors including the photoelectron cross section and the inelastic mean free path of the photoelectrons. Changes in the relative areas of core XPS peaks thus indicate a relative increase or decrease in the amount of various atomic species in different molecular environments.

We observe that the surface chemistry is highly dependent upon the conditions used to prepare the nanoparticles. The overall XPS spectra of all of the samples show that the principal core features can be attributed to C1s, O1s, Na2s, Na2p, Na Auger, S2s, S2p, Cd3d, Cd3p, and Te3d. The metal peaks in some samples are of very low intensity, indicating that the surface of the nanoparticles is largely composed of a capping compound most likely related to mercaptopropionic acid (MPA, $HSCH_2CH_2CH_2COOH$).

The XPS results reveal that the surfaces of the particles are composed largely of Cd, Te, and MPA stabilizer, the latter being responsible for the prevalence of the sulfur peaks. The atomic ratios calculated from peak areas adjusted for photoelectron cross sections show that the metal-to-oxygen ratio in the samples made

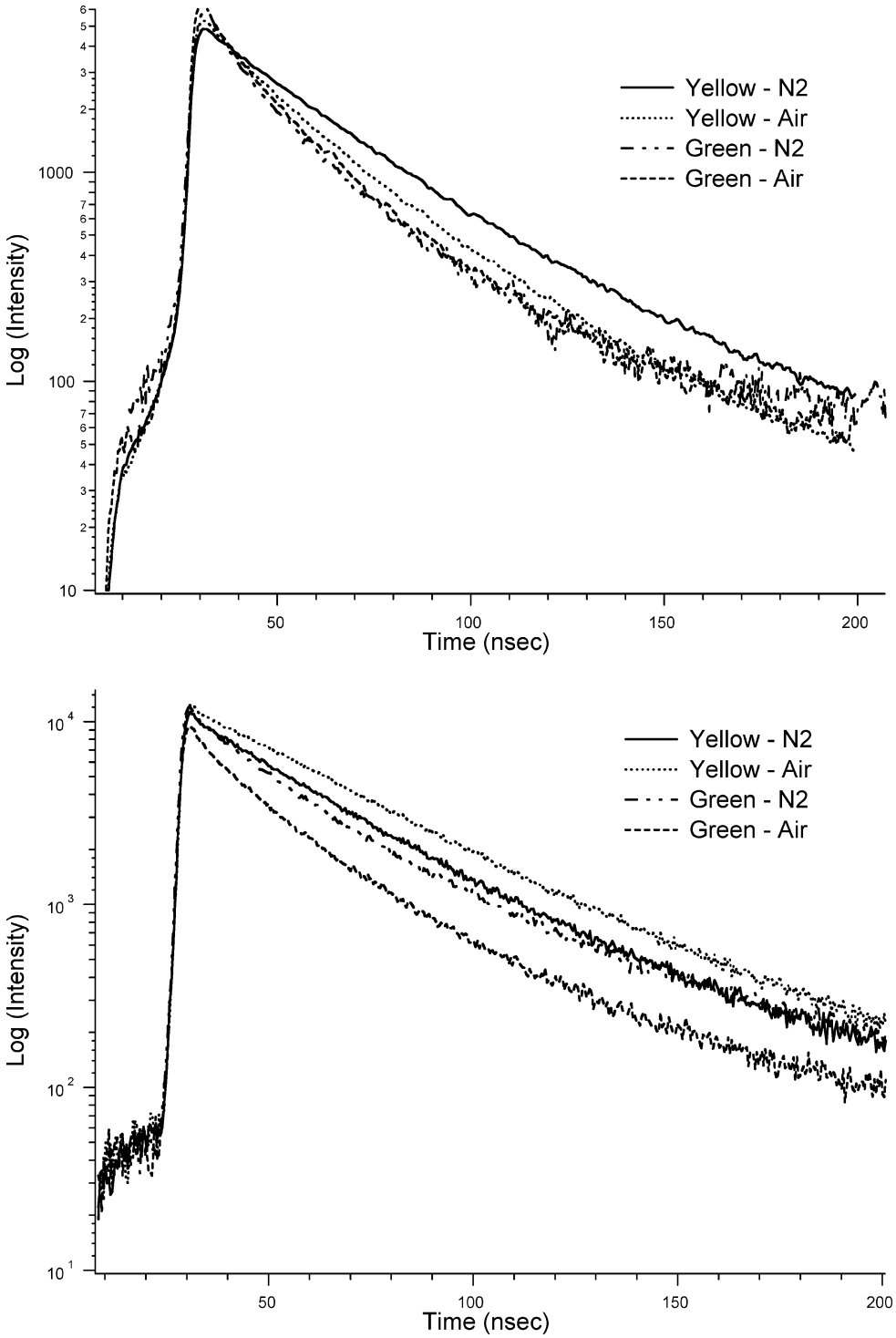

Figure 9. The photoluminescence (top, excitation at 400 nm) and upconversion luminescence (bottom, excitation at 800 nm) decay curves of the green and yellow nanoparticles made in nitrogen and in air.

TABLE 2: Photoluminescence and Upconversion Decay Lifetimes (ns)

	in air		in N_2	
	green	yellow	green	yellow
photoluminescence	18	32	19	24
upconversion	23	37	27	32

in air is much lower that those made in N_2, as shown in Figure 10. This implies that the surface of samples made in air is more oxidized or attached to more oxygen relative to the samples prepared in nitrogen. On the surface, we observe an excess of Cd relative to Te for all samples, and the atomic ratio of Te to Cd does not vary significantly for the samples made in air and in N_2 (0.2−0.4).

The Cd3d and Te3d spectra are displayed in Figure 11. The Cd3d doublet, composed of the $Cd3d_{5/2}$ and $Cd3d_{3/2}$ peaks, is visible in the spectra for all samples. The binding energy for $Cd3d_{5/2}$ is 404.80 eV, and the doublet separation is about 6.70 eV. For the Te3d spectra, however, four peaks are observed. Figure 11 also displays the Te XPS spectrum of Te powder for comparison. The tellurium powder displays two sets of peaks, which can be assigned to the unoxidized (lower energy peaks) and oxidized (higher energy peaks) Te metal. The Te powder displays a high degree of oxidation as determined by the ratio

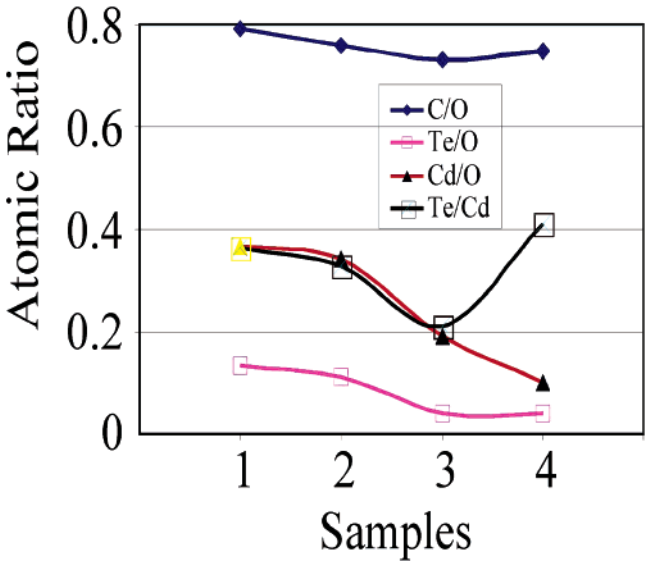

Figure 10. Atomic ratio from XPS peak areas for (1) green sample made in N_2; (2) yellow sample made in N_2; (3) green sample made in air; and (4) yellow sample made in air.

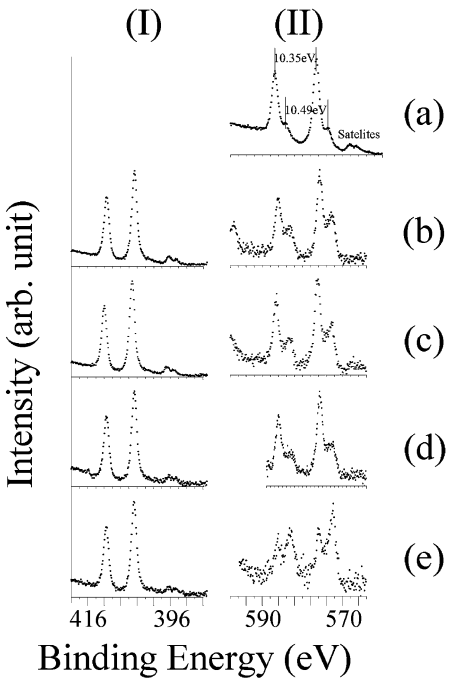

Figure 11. XPS Cd3d (I) and Te3d (II) spectra of nanoparticle samples: (a) Te powder; (b) green sample made in N_2; (c) yellow sample made in N_2; (d) green sample made in air; and (e) yellow sample made in air.

of the peak areas for the oxidized and bare metal species at 576.26 and 573.29 eV ($Te3d_{5/2}$), respectively. The doublet separation is about 10.49 eV for the pure metal species, and 10.35 eV for the oxidized species. The chemical shift between the two species is about 2.99 eV.

In the nanoparticles (Figure 11b−d), the CdTe species shows a peak at 372.7 eV for unoxidized $Te3d_{5/2}$, and for the oxidized Te species the binding energy of the $Te3d_{5/2}$ peak is about 375.50 eV. For most nanoparticle samples, except for the yellow sample made in air (Figure 11e), the oxidized Te peaks have much more intensity than those from CdTe. This result implies that most Te exists as an oxide on the surface. Overall, we do not observe a significant difference in Te oxidation between samples made in air and in N_2 media from the XPS investigation.

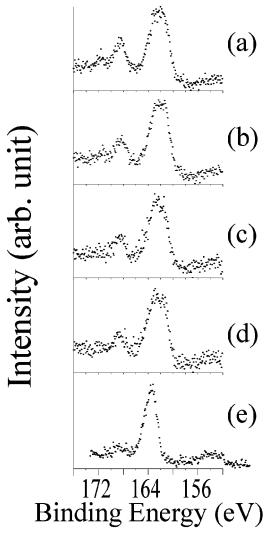

Figure 12. XPS S1s spectra of nanoparticle samples: (a) green sample made in N_2; (b) yellow sample made in N_2; (c) green sample made in air; (d) yellow sample made in air; and (e) MPA stabilizer.

The S2p region is shown in Figure 12 along with a comparison spectrum of MPA. The sulfur XPS spectrum displays two peaks centered around 165 eV, whereas the MPA spectrum consists of only a single peak at about 162.6 eV. The lower binding energy peak of the nanoparticle samples, at 162.6 eV, is consistent with the −S−S− group in MPA, and the higher binding energy feature, at 168.5 eV, can be attributed to oxidized sulfur in groups such as $-SO_2$. The lower binding energy feature at around 154 eV in Figure 12 corresponds to a $K_{\alpha 3\alpha 4}$ satellite feature of the peak at 162.6 eV. The higher binding energy features at 168.5 eV are significantly narrower than the feature at 162.6 eV, a situation that is quite commonly found, as the line width is dependent upon the chemical state of the material. The relative amount of the high binding energy feature at 168.5 eV is higher in the samples made in N_2 than those made in air.

Taken as a whole, the XPS results demonstrate that there is an excess of Cd on the surfaces of the particles and that the samples made in air display a greater degree of tellurium oxidation than those prepared in nitrogen. However, the particles prepared in nitrogen are more likely to have oxidized sulfur groups on the MPA moiety relative to the samples made in air. Thus, it is possible that the small amount of oxygen present during nitrogen synthesis oxidizes primarily the MPA stabilizing agent while greater amounts of oxygen likely result in significant tellurium oxidation.

3.4. Cytotoxicity of Nanoparticles Prepared in Air and in Nitrogen. Figure 13 shows the concentration-dependent reduction in cell viability (using the MTT assay) of CdTe nanoparticles prepared similarly but in either an air or a nitrogen environment. In general, the nanoparticles elicited relatively similar changes in metabolic activity (about 50% maximal reduction in cell viability) regardless of either air/nitrogen conditions or on the relative size of the nanoparticles. Figure 13A shows that synthesis in either air or nitrogen had little apparent effect on the cytotoxicity of CdTe-red particles. With the smaller CdTe-yellow and CdTe-green nanoparticles, there was a suggestion of lesser cytotoxicity with nanoparticles synthesized in nitrogen relative to those synthesized in air (Figure 13B,C). It must be stressed that statistical differences in cytotoxic potential were not demonstrated among any nanoparticle preparations studied.

It is likely that some free Cd^{2+} ions exist in either of these preparations, and free cadmium can be cytotoxic. Derfus and

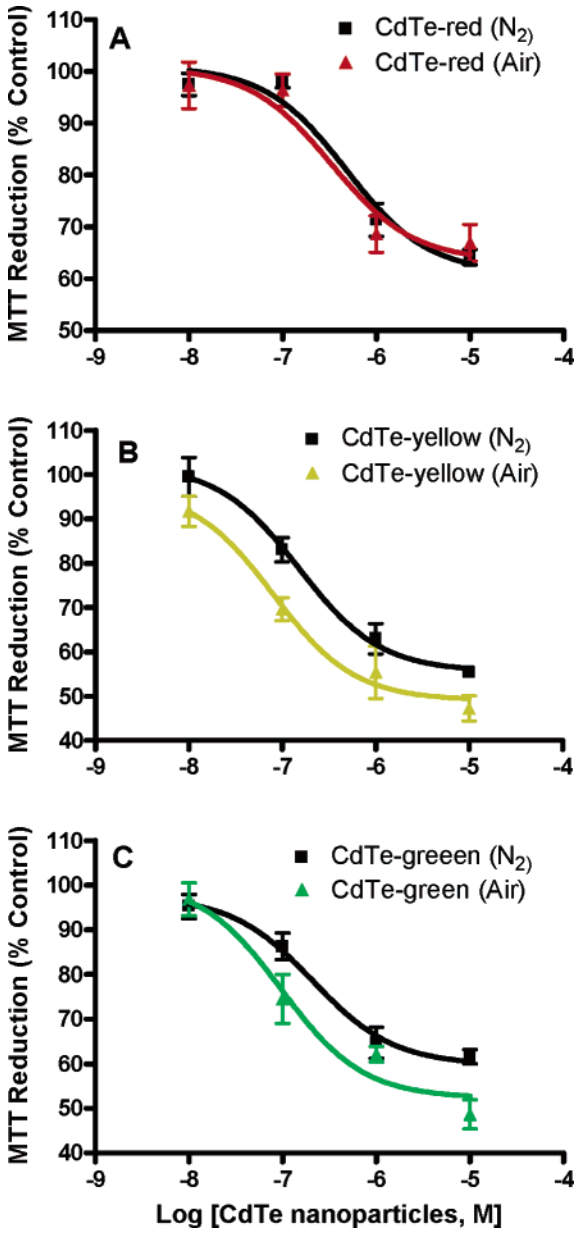

Figure 13. Effect of synthetic conditions (nitrogen or air atmosphere) on cytotoxicity of CdTe nanoparticles. Human hepatoma HepG2 cells were cultured with a range of concentrations of three different sizes of CdTe nanoparticles (red, yellow, or green) made in either nitrogen (N_2) or air. Nanoparticles were added to cells at concentrations of 0, 10^{-8}, 10^{-7}, 10^{-6}, and 10^{-5} M for 24 h prior to evaluating cell viability by the MTT assay. Cell viability was evaluated as affected by exposure to (A) CdTe-red, (B) CdTe-yellow, or (C) CdTe-green nanoparticles synthesized in either N_2 or air. Values represent mean ± SEM of three different experiments with quadruplicates for each concentration of particles.

cowokers[23] suggested the CdSe nanoparticles elicit cytotoxicity at least partially through release of free cadmium ion. In our study, CdTe-yellow and CdTe-green particles made in air appeared slightly more toxic than those made similarly in a nitrogen environment. With synthesis in air, the nanoparticles may be more readily oxidized with release of more free cadmium. XPS analysis also suggests that the oxygen content in the nanoparticles synthesized in air was much higher than that in particles synthesized in N_2. Together, however, these findings indicate that CdTe nanoparticles can be synthesized under either condition with relatively similar physicochemical and cytotoxic properties.

4. Summary

In summary, CdTe nanoparticles made both in air and in nitrogen exhibit strong photoluminescence as well as upconversion luminescence at room temperature. The particles made in air have luminescence comparable to or stronger than that of the particles made in nitrogen, and their decay lifetimes are also similar. The differences between CdTe nanoparticles prepared in air and prepared in N_2 are: (1) the emission half width of CdTe nanoparticles made in air is larger than those prepared in N_2; (2) the particles prepared in air grow faster than the particles prepared in nitrogen; (3) the particles made in air can emit longer wavelengths than the particles made in nitrogen; and (4) the Stokes shift or the phonon coupling in the particles made in air is stronger than in the particles made in nitrogen. XPS analysis suggests that the oxygen content in the nanoparticles synthesized in air is much higher than that in particles synthesized in N_2. With synthesis in air, the nanoparticles may be more readily oxidized with release of more free cadmium. Cytotoxicity studies of the CdTe-yellow and CdTe-green particles made in air display slightly more toxicity than those made similarly in a nitrogen environment likely due to an excess of free cadmium. Together, these findings indicate that CdTe nanoparticles can be synthesized under either condition with relatively similar physicochemical and cytotoxic properties.

Acknowledgment. We would like to thank Nomadics, Inc., the National Institutes of Health (NIH, Grant No. 1R43CA-94403-1 and No. 1R43CA110091-01), the U.S. Army Medical Research Acquisition Activity (USAMRAA) under Contract No. W81XWH-05-C-0101, and partial support by the U.S. Army ERDC-CERL under Contract No. W9132T-06-R-0003. Part of the research described in this paper was performed at the W.R. Wiley Environmental Molecular Sciences Laboratory, a national scientific user facility sponsored by the Department of Energy's Office of Biological and Environmental Research and located at the Pacific Northwest National Laboratory (PNNL). PNNL is operated by Battelle for the U.S. Department of Energy under contract DE-AC06-76RLO1830.

References and Notes

(1) Chen, W.; Joly, G. A.; Wang, S. P. Luminescence of Semiconductor Nanoparticles. In *Encyclopedia of Nanoscience and Nanotechnology*; Nalwa, H. S., Ed.; American Scientific Publishers: Los Angeles, CA, 2004; Vol. 4, pp 689−718.

(2) Gaponik, N.; Talapin, D. V.; Rogach, A. L.; Hoppe, K.; Shevchenko, E. V.; Kornowski, A.; Eychmuller, A.; Weller, H. *J. Phys. Chem. B* **2002**, *106*, 7177.

(3) Mattoussi, H.; Mauro, J. M.; Goldman, E. R.; Anderson, G. P.; Sundar, V. C.; Mikulec, F. V.; Bawendi, M. G. *J. Am. Chem. Soc.* **2000**, *122*, 12142.

(4) Aldana, J.; Wang, Y. A.; Peng, X. *J. Am. Chem. Soc.* **2001**, *123*, 8844.

(5) Willard, D. M.; Carillo, L. L.; Jung, J.; Orden, A. V. *Nano Lett.* **2001**, *1*, 469.

(6) Mitchell, G. P.; Mirkin, C. A.; Letsinger, R. L. *J. Am. Chem. Soc.* **1999**, *121*, 1.

(7) Talapin, D. V.; Rogach, A. L.; Mekis, I.; Haubold, S.; Kornowski, A.; Haase, M.; Weller, H. *Colloids Surf., A* **2002**, *202*, 145.

(8) Talapin, D. V.; Rogach, A. L.; Shevchenko, E. V.; Kornowski, A.; Haase, M.; Weller, H. *J. Am. Chem. Soc.* **2002**, *124*, 5782.

(9) Rogach, A. L.; Kornowski, A.; Gao, M. Y.; Eychmüller, A.; Weller, H. *J. Phys. Chem. B* **1999**, *103*, 3065.

(10) Yu, K.; Zaman, B.; Singh, S.; Wang, D.; Ripmeester, J. A. *Chem. Mater.* **2005**, *17*, 2552.

(11) Klayman, D. L.; Griffin, T. S. *J. Am. Chem. Soc.* **1973**, *95*, 197.

(12) Liang, L.; Qian, H. F.; Fang, N. W.; Ren, J. C. *J. Lumin.* **2006**, *116*, 59.

(13) Morgan, N.; English, S.; Chen, W.; Chernomordik, V.; Gandjbakhche, A.; Russo, A.; Smith, P. *Acad. Radiol.* **2005**, *12*, 313.

(14) Alivisatos, A. P.; Harris, T. D.; Carroll, P. J.; Steigerwald, M. L.; Brus, L. E. *J. Chem. Phys.* **1989**, *90*, 3463.
(15) Gaponenko, S. V. *Optical Properties of Semiconductor Nanocrystals*; Cambridge University Press: New York, 1998.
(16) Gaponenko, S. V.; Woggon, U.; Uhrig, A.; Langbein, W.; Klingshirn, C. *J. Lumin.* **1994**, *60*, 302.
(17) Huang, K.; Rhys, A. *Proc. R. Soc. London, Ser. A* **1950**, *204*, 406.
(18) Leto-Jalil, J.; Perez-Alvarez, R. *Phys. Status Solidi A* **1997**, *164*, 699.
(19) Joly, G. A.; Chen, W.; McCready, E. D.; Malm, J.-O.; Bovin, J.-O. *Phys. Rev. B* **2005**, *71*, 165304.
(20) Wang, X.; Yu, W.; Zhang, J.; Aldana, J.; Peng, X.; Xiao, M. *Phys. Rev. B* **2003**, *68*, 125318.
(21) Cahalan, M. D.; Parker, I.; Wei, S. H.; Miller, M. J. *Nat. Rev. Immunol.* **2002**, *2*, 872.
(22) Chen, W.; Joly, G. A.; McCready, E. D. *J. Chem. Phys.* **2005**, *122*, 22708.
(23) Derfus, A. M.; Chan, W. C.; Bhatia, S. N. *Nano Lett.* **2004**, *4*, 11.